GENERATING RETURN WAVEFORM FOR LLRI ONBOARD CHANDRAYAN-1

BHARAT LOHANI[@], NISHANT BHATNAGAR, ADITYA ROSHAN

Indian Institute of Technology Kanpur, Kanpur-208016, India.

[@]Corresponding author: blohani@iitk.ac.in

***Abstract*— ISRO is launching a LiDAR instrument (LLRI) onboard Chandrayan-I, which will collect topographic data of lunar surface. Time of travel measurement, which is fundamental for topographic coordinate computation, depends upon the shape of return pulse. This shape in turn is a function of the characteristics of footprint, i.e. its geometry, reflectance and roughness. This paper simulates the return waveform from the footprint at the receiver for different conditions within the footprint. Mathematical equations are employed to generate footprints that vary in their characteristics. A footprint is divided into small bins such that each bin has uniform property. Energy distribution over footprint is approximated using the Gaussian distribution of incident pulse. For each bin the energy incident is computed and accordingly the reflected energy is determined. The final waveform is generated by integrating the energy returned from all the bins. Results are presented to show the performance of the developed system.**

I. INTRODUCTION

Chandrayan-I, an Indian lunar mission, will carry a spaceborne altimetric system named LLRI (Lunar Laser Ranging Instrument) for measuring the topography of lunar surface. The LLRI is a high altitude LiDAR (Light Detection And Ranging) system, which will measure the time of flight of the laser pulse. The time of flight measurement depends upon the shape of return pulse which is distorted due to the variations within the footprint. Therefore, the shape of the received waveform contains important information about surface roughness, slope and reflectivity. There is a need to understand, how the LLRI will register the waveform for a given terrain and the relationship between instrument's specification, performance and the terrain characteristics. This paper attempts to simulate the effect of variation in the characteristics of the terrain on the return waveform generated by LLRI.

II. METHODOLOGY

The simulator developed generates complete waveform for a given footprint by the use of mathematical modeling. To achieve this objective, the process of data generation is carried out using the steps shown in Figure 1 and discussed below.

A. Terrain modeling and Tessellation

The terrain can be represented either by a continuous function such as $z=f(x, y)$ or in a discrete manner as in case of a raster. The approach followed in the present case is to divide the footprint into smaller units and then to compute the power incident on their centroid. Therefore, there is a need to discretise the surface into a set of smaller surface elements, wherein the terrain characteristics can be assumed uniform.

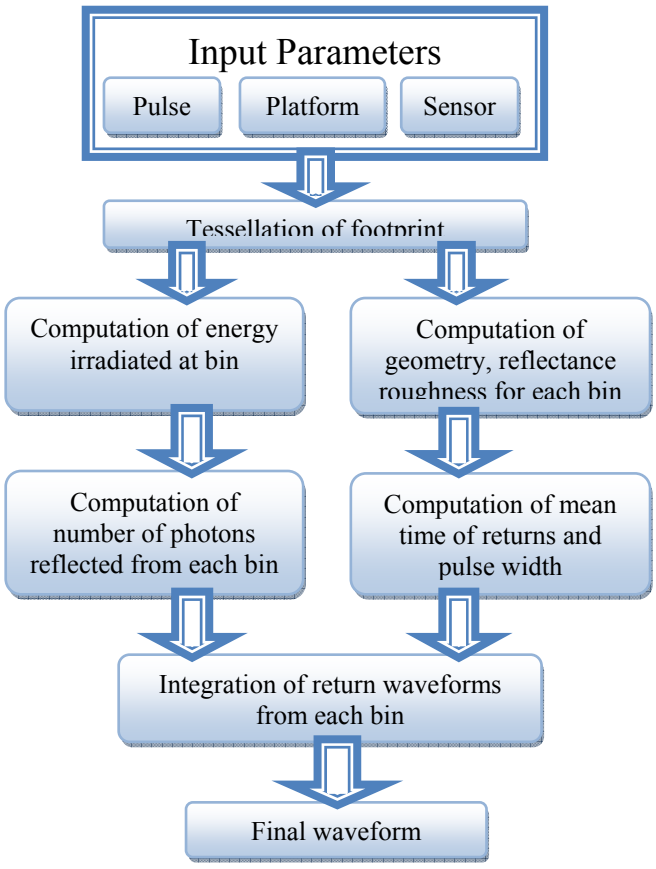

Figure 1: Flow chart showing the methodology

For discretising the entire footprint into small equally sized bins, the footprint is first divided into concentric circles with a user specified constant increase in the radius. Circumference of each circle is then divided into equal parts (equal to *4(n+1),* where *n* is the number of the concentric circle from the centre). The points resulting from the above are then joined to form planer simplexes. In order to create optimal size triangles, the Delaunay triangulation method has been used. The triangles (planar simplexes) formed by Delaunay triangulation are termed as 'Bins', as shown in Figure 2. Considering that the bins are small a uniform energy distribution is assumed within these. Selection of different functions *z=f(x,y)* provide different kinds of surfaces for the footprint.

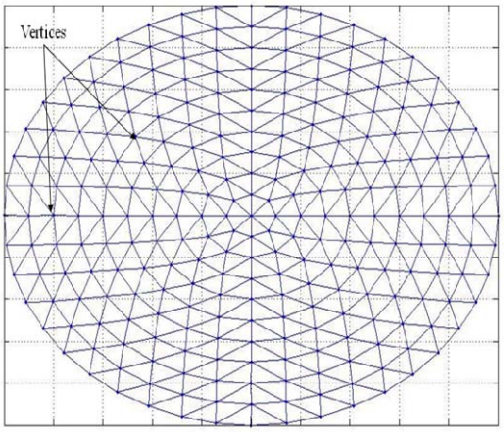

Figure 2: Division of the footprint in small triangular bins

The energy distribution in *XY* plane remains constant irrespective of the relief variation within the footprint. Thus, only the projected area of the bin is considered, i.e. area in *XY* plane, on which power is incident.

Let the coordinates of three vertices forming a simplex are (x_i, y_i, z_i), where $i=1..3$ and $z_i=f(x_i, y_i)$. (x_i, y_i) are known from the discretisation process discussed above. The equation of the simplex is given by $ax + by + cz + d = 0$ where the coefficients '*a*', '*b*' and '*c*' are computed as:

$$\begin{aligned} a &= y_1(z_2 - z_3) + y_2(z_3 - z_1) + y_3(z_1 - z_2) \\ b &= z_1(x_2 - x_3) + z_2(x_3 - x_1) + z_3(x_1 - x_2) \\ c &= x_1(y_2 - y_3) + x_2(y_3 - y_1) + x_3(y_1 - y_2) \end{aligned} \quad (1)$$

The equation of plane formed by the bin can be written as $Z = -((a/c)x + (b/c)y + d/c)$. The mean time of travel $E(t_p)$ and the mean square pulse width $E(\sigma_p^2)$ for each bin (shown in appendix A), are dependent upon the angle made by the bin with *X* and *Y* axes, i.e. *Sx* and S_x respectively. These are computed as $S_x = a/c$ and $S_y = b/c$.

After dividing the footprint into small bins, their radial distance 'r' from the centre of footprint is computed as:

$$r = \sqrt{x_{cent}^2 + y_{cent}^2} \quad (2)$$

Where x_{cent} and y_{cent} are the coordinates of centroid of the bin and are computed as:

$$\begin{aligned} x_{cent} &= \frac{x_1 + x_2 + x_3}{3} \\ y_{cent} &= \frac{y_1 + y_2 + y_3}{3} \end{aligned} \quad (3)$$

Similar to geometry, the reflectance variation is implemented by considering it as a function of the coordinates of the bin under consideration, i.e. $\rho = g(x,y)$. The function $g(x,y)$ can be continuous or a raster.

The pulse width of the return pulse also depends on the surface roughness, which is assumed Gaussian with mean being zero and is expressed as:

$$F_s = \frac{1}{\sqrt{2\pi\sigma_s}} e^{-\frac{1}{2}\left(\frac{s}{\sigma_s}\right)^2} \quad (4)$$

Where, σ_s is the measure of spread of roughness with a mean of zero. F_S is computed for $-3\sigma_s \le s \le +3\sigma_s$. The roughness value '*s*' at each bin is so decided that it satisfies the frequency distribution given by the above equation and also that these do not have any spatial autocorrelation in *XY* plane.

B. Energy incident on footprint

The pattern of intensity distribution across the width of laser pulse is considered TEM_{00} (Transverse Electromagnetic) which has a Gaussian profile given by:

$$I(r_i, z) = \frac{2P_t}{\pi w_z^2} e^{-2\left(\frac{r_i}{w_z}\right)^2} \quad (5)$$

Where $I(r_i, z)$ is the intensity function, P_t is the total power transmitted , w_z is the beam radius at a distance of 'z' from the point of origin of laser and ri is the radial distance from the axis of laser to the ith bin's centroid. The total power incident on footprint can be computed by $P_t = \sum(Api \times I(r_i,z))$ where *Api* is the projected area of the ith bin and $I(r_i, z)$ is the intensity of the pulse at a radial distance of ri from the centre as shown in Figure 3. As the intensity depends on *'z'*, the variation in intensity due to change in elevation within the footprint is also taken into account. For this, the '*z*' is considered as the vertical distance between the centroid point of bin and the sensor.

C. Computing the waveform

The present simulator is designed considering that the photons reach the receiver over a period of time from a bin. This Gaussian waveform has an area equal to the number of photons incident on the bin with the mean as the expected time of travel $E(t_p)$ and the standard deviation as the square root of mean pulse width $\sqrt{E(\sigma_p^2)}$ (appendix A). The final waveform is formed by integrating the waveforms obtained from each bin.

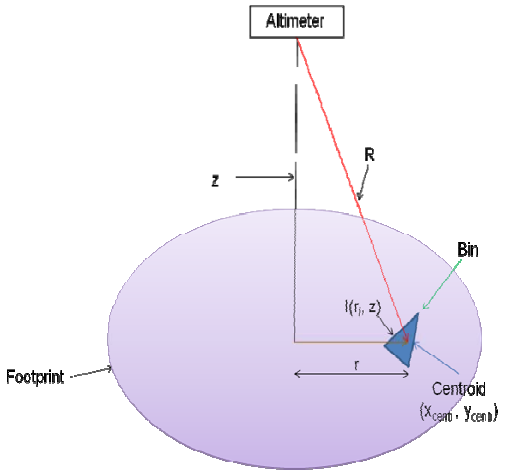

Figure 3: Relationship of altimeter, footprint and bin

To account for the maximum number of photons being received, extent of the waveform is taken as ±4σ.

$$\text{Where, } \sigma = \sqrt{E(\sigma_p^2)}$$

To compute the amplitude '*Amp*' of the waveform for a single bin, equation of the Gaussian waveform $G(\mu, \sigma^2)$ is:

$$G(\mu,\sigma^2) = Amp \times e^{-\frac{1}{2}\left(\frac{t-\mu}{\sigma}\right)^2} \qquad (6)$$
$$\text{where } \mu = E(t_p) \text{ and } \sigma = \sqrt{E(\sigma_p^2)}$$

Next, the Gaussian is integrated between the limits $\mu - 4\sigma$ and $\mu + 4\sigma$ to obtain the area under the curve. The area under the Gaussian curve is equal to the number of photons (N_i) actually reaching the receiver after reflection and transmitting through the atmosphere, which is computed using the following link equation:

$$N_i = \left[\frac{E}{h\nu}\right]\left[\frac{A_{reciever}}{z^2}\right]\left[\frac{\rho}{\Omega_{surface}}\right]\Gamma_{sys}\Gamma_{atm}^2 \qquad (7)$$

Therefore,

$$N_i = \int_{\mu-4\sigma}^{\mu+4\sigma} Amp \times e^{-\frac{1}{2}\left(\frac{t-\mu}{\sigma}\right)^2}$$

And,

$$Amp = \frac{N_i}{\int_{\mu-4\sigma}^{\mu+4\sigma} e^{-\frac{1}{2}\left(\frac{t-\mu}{\sigma}\right)^2}}$$

The parameters of Gaussian pulse reaching the receiver from each bin are thus determined as μ, σ and *Amp*. The final waveform is computed by integration of intensities of pulses from bins with respect to time. A Matlab based program is written to realize the above steps.

III. Results

Results obtained for different characteristics of footprint are presented in this section. The sensor and pulse characteristics are taken from the LLRI specifications as shown in Table 1. Results presented here (Figure 4 to Figure 8) are generated considering the reflectance within footprint as 1 and roughness as 0.5m. While plotting the waveforms it is attempted to use the same ordinate scales for similar kinds of results. However, changes in these from one set of result to other are due to the intention to show the waveform in best possible manner.

TABLE 1
SPECIFICATIONS OF LLRI

Orbital altitude	100,000m	System transmission	0.5
Energy	50 mJ	Atmospheric transmission	0.5
Laser wavelength	1064nm	Receiver impulse response	0 s
Pulse width	10ns	Laser type	Nd-YAG Diode Pumped Q switched laser
Beam Divergence	0.5mrad		
Telescope receiver area	0.0725 m^2	Speed of light	2.997925×108 m/s
Radius of footprint	50 m	Plank constant	6.625×10-34 J/s

To check the accuracy of simulator, the total number of photons reaching the altimeter is computed theoretically using link equation (7) as 77196. The same was determined by computing the area under the return waveform as 66868 from the simulator. The relative difference between these is:

$$\frac{77196-66868}{100} * 100 = 13.38\%$$

The difference in the number of photons can be attributed to the fact that the theoretical computation assumes a step pulse within the footprint. However, the fired pulse is Gaussian and a small portion of energy also falls outside the footprint (the footprint in simulator is considered only up to the $1/e^2$ divergence limit), which results in lower number of photons.

Figure 4 shows the return waveforms for three different inclinations of a planar surface. With the increase in inclination the waveform for two different kinds of stepped surfaces within amplitude decreases and pulse width increases. Besides showing the return waveforms these results also corroborate the performance of simulator, as the outcomes are obvious. Figure 5(a and c) show the return the footprint. In the first case the resulting waveform shows first peak for the central elevated part while the second peak is for the lower surface on edges. The amplitudes of return peaks are different due to the fact that the intensity of transmitted pulse is sufficiently larger at its center. Further, the time difference in arrival of these pulses is (0.000667128338658681 - 0.000666827973153382) 0.30037 microseconds, which is equivalent to 90m length. As the difference in height of these two steps is 45m (two way distance 90m) the resulting waveform shows the accuracy of developed system. In the second case Figure 5(c) shows that the amplitude of resulting peaks are nearly same. The minor difference is due to the extra distance, thus more atmospheric absorption that the pulse suffers for the lower half. Similar to Figure 5 (a), here also the difference in arrival time of pulses of 0.3 microseconds, which is according to the height difference. The returns for both peaks in above case are Gaussian despite the pulse being split in half in transverse direction. This is because the pulse is also Gaussian in longitudinal direction. In Figure 5 (b and d) the surfaces of Figure 5 (a and c) are made rough by changing the elevation value as $z_n = z + 5sin(x)cos(y) + 2cos(x)sin(y) + 5$, where z_n is the new elevation value at (x,y). The resulting surface is rough thereby altering the slopes of bins in different directions. Also, noticeable is the increase in pulse width for both peaks. These changes result in lower amplitude return at receiver, though the separation between peaks remains same as original surfaces.

Figure 6 shows the return waveform for a footprint having a stair type surface with five steps. The tread and rise of steps are 20m and 80m, respectively. Time difference between each echo is approximately 0.5335814 microseconds which is total pulse travel time. The height of each step is given by half of time difference between each pulse. The distance corresponding to 0.2667907 microseconds is approximately 79.98 meter, which is very near to the rise of step.

Figure 7 (a) shows the return waveform for a footprint with two inclined surfaces. In Figure 7 (b) the waveform is shown for erected hemispherical footprint. The aim of showing these results is to show the versatility of simulator and also to understand how the waveform will appear for different footprints. The simulator can also generate a footprint having a natural looking surface (fractal surface generated using diamond algorithm) and simulate the waveform, though the results are not shown here. The simulator can create surfaces with variation in geometry, reflectance and roughness within a single footprint, as shown in Figure 8.

The simulator further helps in understanding the behavior of laser pulse interaction with the footprint. Different return waveforms were generated for a flat surface by varying the footprint parameters. As shown in Figure 9 (a and b), the total number of photons returned and the amplitude of return waveform have a liner relationship with the reflectance. With the increase in surface angle, the amplitude reduces and pulse width increases as shown in Figure 10 (a and b). This is obvious, as the irradiance of incident laser pulse reduces due to increase in area of footprint. Increasing the amplitude of surface roughness causes the footprint surface to have more effective area which spreads the incident pulse more and results in lower amplitude and large pulse width (Figure 11(a and b)).

IV. Conclusion

A LiDAR return waveform simulator has been developed. Results are presented considering the LLRI parameters. This simulator can be used for other LiDAR systems by changing the parameters. Return waveforms have been generated for various kinds of footprints. The performance of the simulator has been checked through theoretical computation and has been found satisfactory. Results generated by this simulator also match with the published results[1] when the same parameters are employed. Although, the system developed in [1] simulates return waveform for only planer surfaces. It is intended to carry out further validation with experiments with actual LiDAR sensor. At present the simulator generates return waveform only for the photons received at the receiver. However, with more information on sensor characteristics it will be possible to generate the final voltage versus time curves which are actually employed for multiple return measurements. This work opens further research scope to determine footprint characteristics from a given return waveform though the reverse modeling is not a straightforward step.

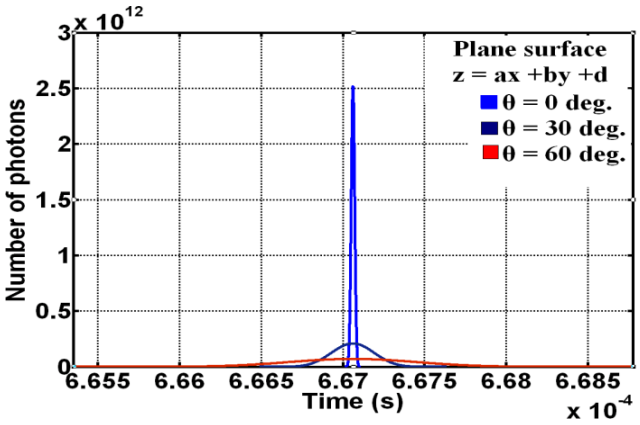

Figure 4: Return waveform for a plane surface at different angles

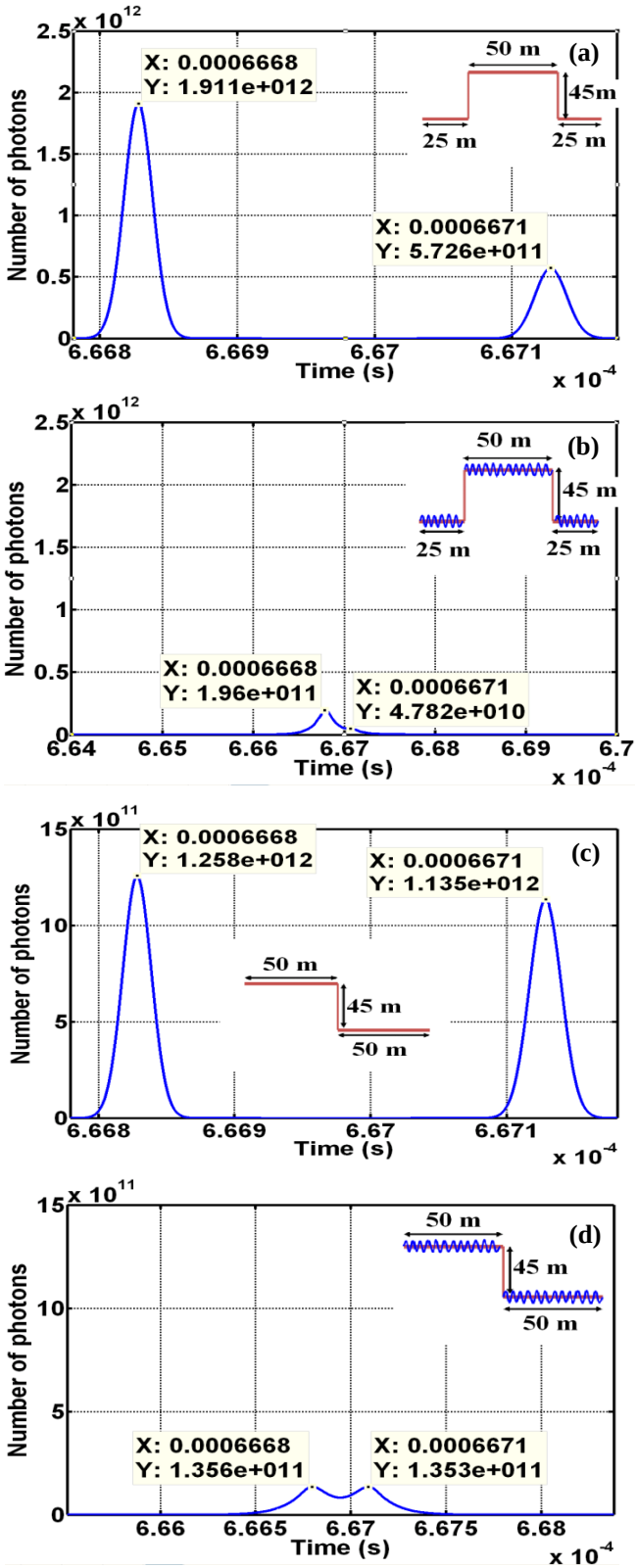

Figure 5: Return waveforms for a two stepped footprint without and with undulations.

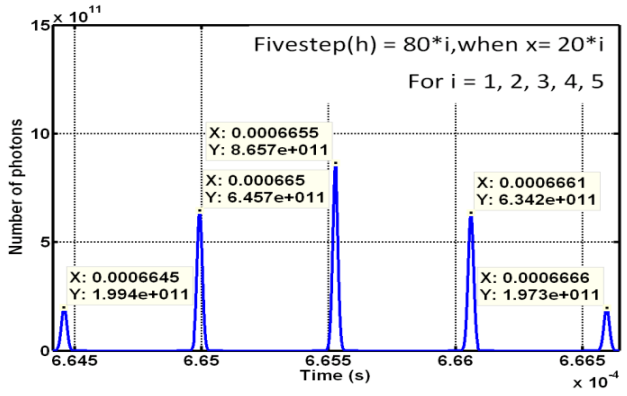

Figure 6: Return waveform for 5 step footprint

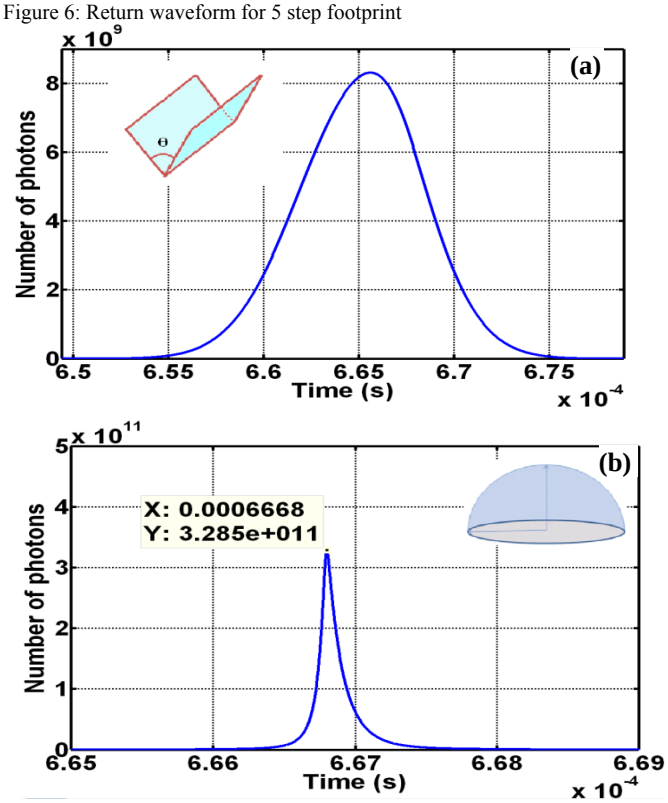

Figure 7: Return waveform for different shaped footprint -- (a) two inclined plane, (b) erected hemisphere

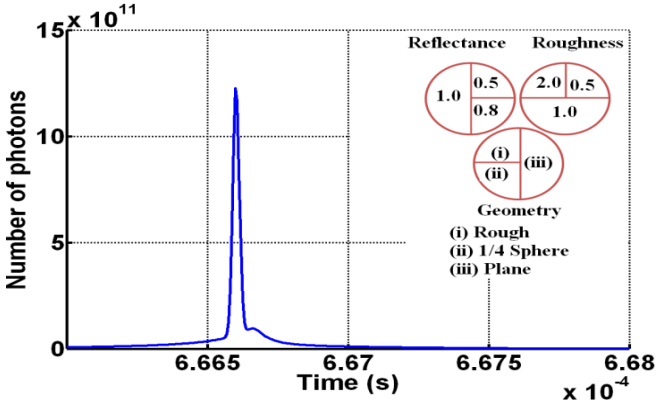

Figure 8: Return waveform for a complex footprint with variation of geometry, reflectance and roughness

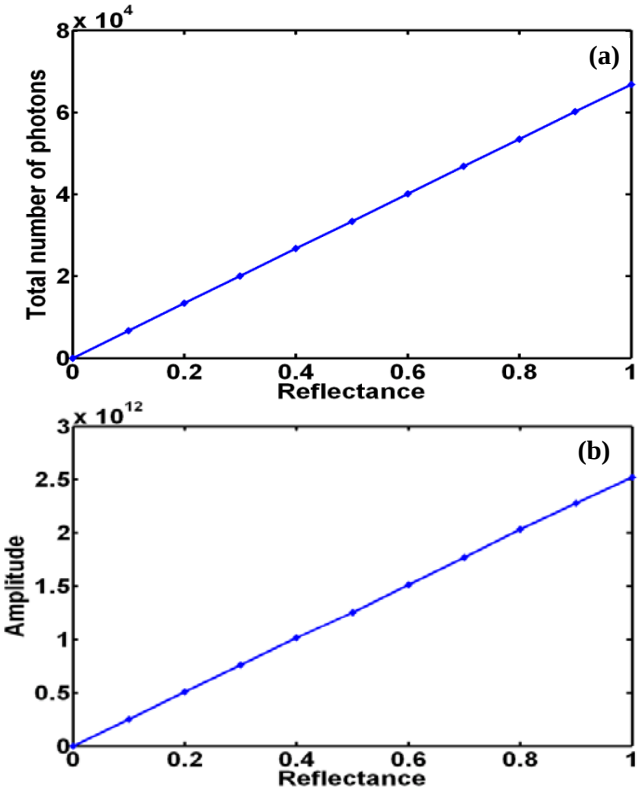

Figure 9: The effect of change in reflectance of surface on return waveform energy and amplitude

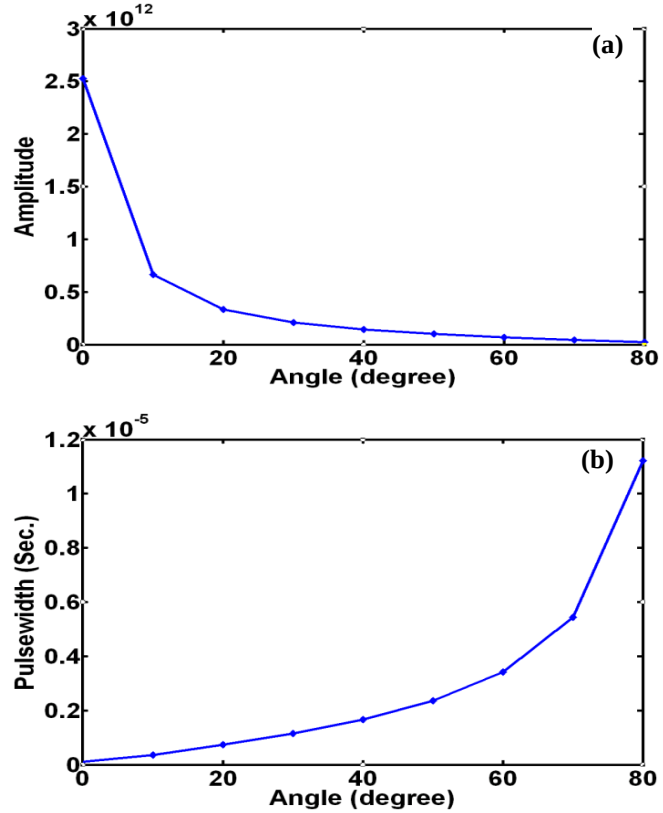

Figure 10: The effect of change in angle of surface on the return waveform amplitude and pulse width

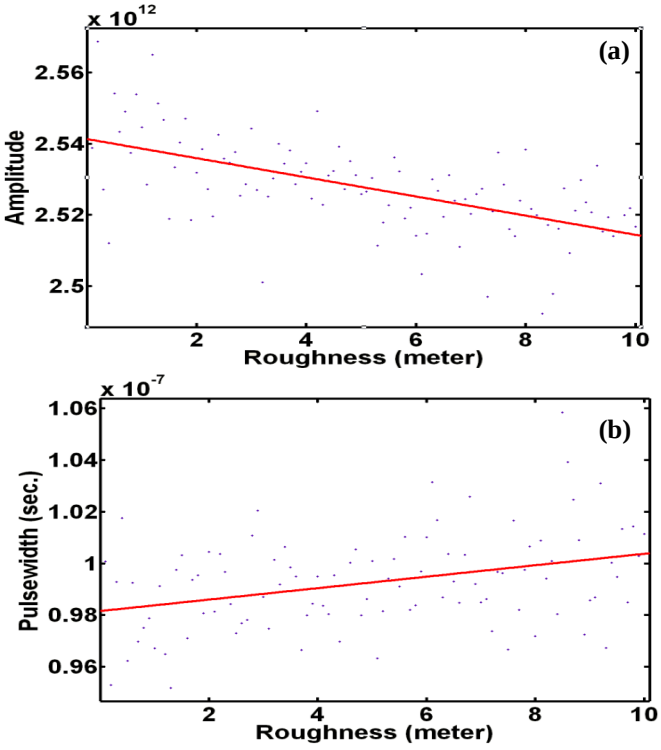

Figure 11: Effect of roughness on amplitude and pulse width of returned waveform

ACKNOWLEDGEMENT

Authors thank ISRO-IITK cell for funding this work. Dr. J Kamlakar, LEOS, ISRO provided necessary feedback and data for this work.

APPENDIX A

The expected value of travel time $E(t_p)$ and root mean square pulse width for a Gaussian laser pulse $E(\sigma_p^2)$ is given by [2] as shown below.

$$E(t_p) = \frac{2R(1+\tan^2\theta)}{c\times\cos\phi}\left[1+(1+2\tan^2(\phi+S_x))\frac{\mathrm{var}(\Delta\phi_x)}{2} + \cos^2\phi\left[1+\frac{2\tan^2 S_y\cos^2 S_x\,\mathrm{var}(\Delta\phi_y)}{2\cos^2(\phi+S_x)}\right]\right]$$

$$E(\sigma_p^2) = \sigma_l^2+\sigma_h^2+\frac{4\,\mathrm{var}(S_t)\cos^2 S_x}{c^2\cos^2(\phi+S_x)} + \frac{4R^2\tan^2(\theta)}{c^2\cos^2(\phi)}\left[\tan^2\theta+\tan^2(\phi+S_x)+\frac{\tan^2 S_y\cos^2 S_x}{\cos^2(\phi+S_x)}\right]$$

Where

t_p	travel time estimated by pulse centroid
σ_p	RMS received pulse width
σ_l	RMS transmitted pulse width
σ_h	RMS width of receiver impulse response
c	velocity of light
S_t	surface roughness
φ	off nadir angle
S_x	surface slope in xz plane
S_y	surface slope in yz plane
R	altimeter altitude
θ	half width of divergence angle
$\Delta\varphi_x$	pointing error parallel to pointing direction
$\Delta\varphi_y$	pointing error normal to pointing direction

REFERENCES

[1] Filin Sagi, Csathó Bea, 2000. "An efficient algorithm for the synthesis of laser altimeter waveforms". *BPRC technical report,* pp. 1-27

[2] Gardner, C. S., 1982. "Target signatures for Laser altimeters: an analysis". *Applied optics*, Vol. 21, No. 3, 1st February 1982.